Using Magnetic Levitation for Three Dimensional Self-Assembly

*Katherine A. Mirica, Filip Ilievski, Audrey K. Ellerbee, Sergey S. Shevkoplyas, and George M. Whitesides**

The development of practical strategies for the assembly of objects into 3D arrays is an unsolved problem. This paper describes the use of magnetic levitation (MagLev) to guide the self-assembly of millimeter- to centimeter-scale diamagnetic objects, which we call "components", each programmed by shape and distribution of density, into 3D assemblies and structures in a paramagnetic fluid medium positioned in the magnetic field gradient generated by NdFeB magnets. When the components are not in contact, their equilibrium configuration depends on the balance of magnetic and gravitational forces they experience. This technique provides a convenient method to position components in 3D without mechanical contact; we demonstrate its unique capabilities using components with optical functions, and with components that form ordered, assembled structures when transferred into contact with solid supports.

Most functional devices are assembled from components (by either humans or machines) and connected mechanically. The ability to carry out any part of these processes automatically, or even to preposition or preorient the components reliably, would simplify them. Self-assembly is a useful technique for generating ordered assemblies,[1–3] and although there are exceptions, it has been most highly developed when the components are all the same, and when there is a (quasi) 2D template (e.g., surface) to guide the process.[3–5] We and others have demonstrated self-assembly across a range of sizes,[6–14] and have also generated self-assembled functional structures,[3,15–25] albeit with limited practical utility. Here, we introduce a very flexible strategy that uses magnetic and gravitational forces for arranging components in 3D.

The use of the magnetic force is a versatile strategy for guiding self-assembly.[7,26–28] Approaches towards self-assembly based on magnetic interactions are particularly convenient because: i) magnetic forces act at a distance and, therefore, enable contactless manipulation of objects; ii) the spatial distribution of the magnetic forces is straightforward to program and to vary using arrays of magnets and electromagnets; and iii) a globally applied magnetic field is capable of addressing a large number of components in parallel.

Current approaches that use the magnetic force for self-assembly can be subdivided into two categories. The first, more common, approach relies on the use of permanent magnets and electromagnets to control, manipulate, align, actuate, and assemble components containing embedded ferromagnetic elements.[7,26–28] Although this approach is common, it is limited to components capable of strong magnetic interactions, i.e., components typically containing the elements Ni, Co, and/or Fe. The second, less common, approach is based on MagLev, a method that suspends diamagnetic objects, i.e., objects that lack permanent magnetic moments and unpaired electrons, against gravity using a counterbalancing magnetic force. Since diamagnets encompass a much wider variety of materials than ferromagnets, including most organic substances, water, and plastics, MagLev represents an underexploited, but potentially very versatile and widely applicable strategy for contactless manipulation and assembly of objects in 3D.

Examples of MagLev exist in vacuum,[29,30] air,[31–36] in liquid[37] and pressurized[38–40] oxygen, in solutions of paramagnetic ions,[41–48] and in suspensions of ferromagnetic particles in a carrier fluid[49] using various sources of the magnetic field, e.g., permanent magnets, simple electromagnets, and superconducting magnets. Initial demonstrations of MagLev were limited to the levitation of strongly diamagnetic materials, such as pyrolytic graphite and bismuth, using permanent magnets or electromagnets in air or under vacuum.[29,30,34,36,50] Despite its limitation, this concept found a number of applications during the 1960s, including a frictionless rotor,[36] accelerometer,[51] a tiltmeter/seismometer,[34] and a pressure gauge.[29] During the 1960s and 1970s applications of MagLev extended to density-based analyses and the separation of minerals, metals, and plastics suspended in paramagnetic fluids using permanent magnets and electromagnets.[41] Subsequent use of superconducting and Bitter-type magnets in the 1990s and 2000s expanded the range of materials that could be suspended against gravity to include wood, glass, gold, water, ethanol, living organisms, and many other samples.[31,32,35,37–40,52–59] The discovery of NdFeB magnets, followed by their widespread commercial availability, enabled many of the most recent applications of MagLev in density-based chemical analysis,[44–46,48] separation,[48] and

Dr. K. A. Mirica, Dr. F. Ilievski, Prof. A. K. Ellerbee, Prof. G. M. Whitesides
Department of Chemistry and Chemical Biology
Harvard University
12 Oxford St., Cambridge, MA 02138, USA
E-mail: gwhitesides@gmwgroup.harvard.edu
Prof. G. M. Whitesides
Wyss Institute for Biologically Inspired Engineering
Harvard University
3 Blackfan Circle, Boston, MA 02115, USA
Prof. S. S. Shevkoplyas
Department of Biomedical Engineering
Tulane University
500 L. Boggs Building, New Orleans, LA 70118, USA

DOI: 10.1002/adma.201101917

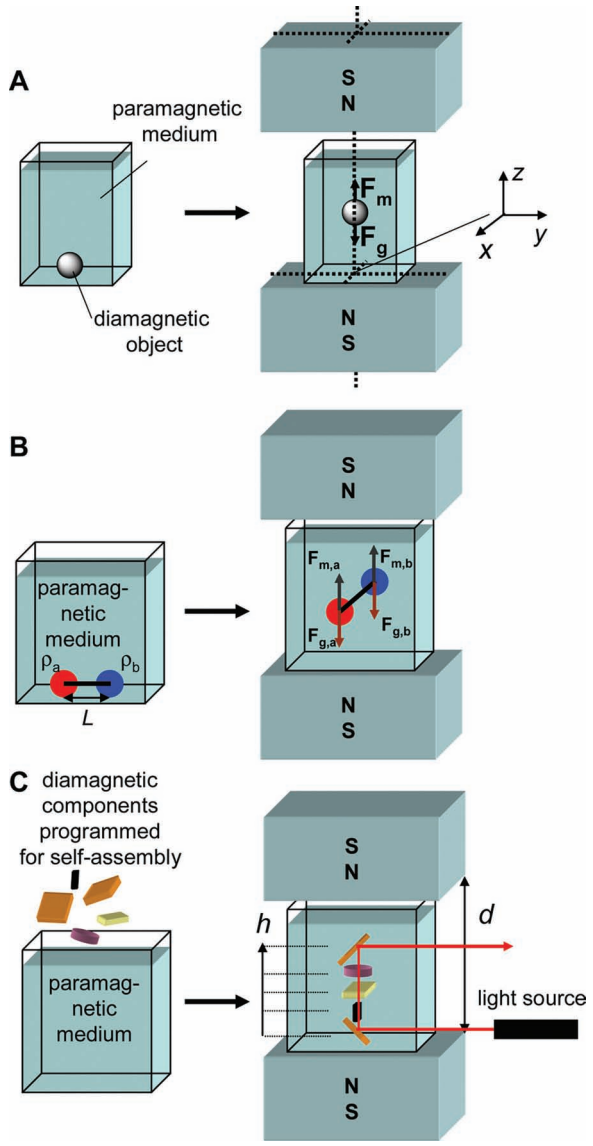

Figure 1. Experimental design for MagLev. A) The balance of magnetic (F_m) and gravitational (F_g) forces determines the vertical equilibrium position of an object levitating within the MagLev device. B) The distribution of densities within an object can be used to program its tilt angle during magnetic levitation. C) Schematic of a complex assembly with designed function where each component levitates in a specific 3D configuration determined by the magnetic and gravitational forces acting on it.

contactless manipulation and trapping of diamagnetic objects in 3D.[33,43,48,49,60,61] This paper uses the established principles of MagLev to develop an approach for self-assembly of diamagnetic objects in 3D with unprecedented control over many aspects of position and orientation of components.

Figure 1 summarizes the principles that underlie MagLev.[31,37–39,41,44–46,48,49] The device used is simple: two permanent magnets oriented with like poles facing each other (in an anti-Helmholtz configuration) and separated by a container containing a paramagnetic medium (here an aqueous solution of $MnCl_2$).[44–46,48,62] The conditions for static equilibrium in MagLev require that for each object: i) the net force acting on the object equals zero (Equation 1) and ii) the net torque around any arbitrary pivot point equals zero (Equation 2). In these equations, $\vec{F}_g$ (N) is the force of gravity, $\vec{F}_m$ (N) is the magnetic force acting on the object, and $\vec{r}$ is the lever arm vector (a vector from the pivot point to the point of application of force).

$$\vec{F}_g + \vec{F}_m = \vec{0} \tag{1}$$

$$\vec{r} \times (\vec{F}_g + \vec{F}_m) = \vec{0} \tag{2}$$

To simplify the derivations, we approximate an object of heterogeneous density as a composite object (subscript c) comprising two non-overlapping parts (subscripts a and b) of homogeneous densities whose centers of mass connect by a massless rod of length L(m). We assume that the magnetic susceptibilities of the two parts of the composite object are identical. In a 3D Cartesian coordinate system in which the Z-axis is aligned with the direction of the vector of gravity and coincides with the centerline (the line connecting the centers of the two magnets), the origin is in the center of the top surface of the bottom magnet, and the YZ-plane contains the centers of mass of both parts of the composite object. Equation 3 gives h (m), the distance between the top surface of the bottom magnet and the center of volume of the object (the "levitation height" of the composite object), and Equation 4 gives θ, the angle of tilt of the composite object in the YZ-plane, defined as the angle between the Z-axis and the link connecting the centers of mass of the two components comprising the object.

$$h = \frac{d}{2} + \frac{(\rho_c - \rho_m)\, g\, \mu_0}{\alpha_z^2\, (\chi_c - \chi_m)} \tag{3}$$

$$\theta = \cos^{-1} \frac{(\rho_b - \rho_a)\, g\, \mu_0}{(\chi_c - \chi_m)\left(\alpha_y^2 - \alpha_z^2\right) L} \tag{4}$$

In these equations, ρ_a (kg m^{-3}) and ρ_b (kg m^{-3}) are the densities of the two parts of the composite object, ρ_c (kg m^{-3}) is the average density of the composite object, ρ_m (kg m^{-3}) is the density of the paramagnetic medium, χ_c (unitless) is the magnetic susceptibility of the object, χ_m (unitless) is the magnetic susceptibility of the paramagnetic medium, g (m s^{-2}) is the acceleration due to gravity, $\mu_0 = 4\pi \times 10^{-2}$ (N A^{-2}) is the magnetic permeability of free space, d(m) is the distance between the magnets, α_y is the gradient of the Y-component of the magnetic field along the Y-axis, and α_z is the gradient of the Z-component of the magnetic field along the Z-axis. The Supporting Information provides a derivation and a detailed account of the assumptions and simplifications associated with these equations.

We use these requirements for static equilibrium to organize the components in 3D. We control the gravitational force acting on an individual component by controlling the average density of the component and the density of the fluid and by patterning the distribution of density within the component. For a particular system with fixed values of magnetic parameters (magnetic field and magnetic field gradient, magnetic susceptibilities) and a medium of constant density, the average density of an object of heterogeneous density determines its

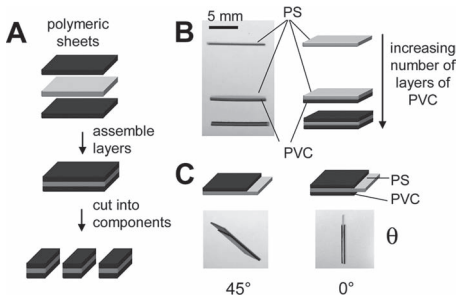

Figure 2. Programming the vertical position and orientation of components using patterns of density. A) A method for patterning density using stacked layers of polymer sheets and tape cut by a laser. B) Photographs of three squares of different densities levitating in 1 M $MnCl_2$ (left panel). The squares were fabricated from planar layers of polystyrene (PS) and polyvinyl chloride (PVC) tape with an adhesive backing. C) Schematic representations and photographs showing side views of two squares programmed to levitate in different configurations in 1M $MnCl_2$ (i.e., tilted (45°) and vertical (0°)) using specific density patterns of PS and PVC tape. Each square is 10 mm × 10 mm.

levitation height at equilibrium (Equation 3); the pattern of density within the object defines the orientation of the object relative to the axis of gravity (Equation 4). We use the gradient of magnetic field, and the densities of the components, to control the vertical and lateral position of levitating objects, as well as their orientation.

Figure 2A sketches the method we used to fabricate millimeter-sized components with preprogrammed densities. For our demonstrations, we used stacked layers of different polymers (e.g., commercially available tapes and polymeric sheets) bonded with thin layers of adhesive to pattern the density of the components. We then used a laser cutter to fabricate the shapes. Figure 2B demonstrates control over the vertical position of square slabs (10 mm on a side). Tape (polyvinyl chloride, PVC, $\rho = 1.40$ g cm^{-3}) introduced dense regions onto the surface of polystyrene (PS, $\rho = 1.05$ g cm^{-3}). The number of layers of tape (Figure 2B, right panel) determined the mean density and the height of levitation of each square.

Patterning the density of a slab controls its orientation relative to the gravitational vector (Figure 2B,C). Flat squares with a uniform pattern of density along their square face orient perpendicular to the vector of gravity (Figure 2B). Figure 2C shows that patterning the square with PVC tape controls its orientation relative to the gravitational vector. The average density of the square determines its vertical position above the bottom magnet, and the distribution of densities on the square determines its tilt angle.

Gravitational force is uniform over the entire volume of the container. Magnetic force directs the diamagnetic objects suspended in a paramagnetic medium away from regions of higher magnetic field towards regions of lower magnetic field; the direction of the magnetic force is along the gradient of magnetic field. Gradients of the magnetic field, therefore, allow diamagnetic objects to be positioned and aligned. Two easily manipulated parameters affect the gradient of the magnetic field: i) the shape of the magnets and ii) the distance (d) between them.

Using magnets of different shapes controls the alignment of levitating objects in the *XY*-plane. **Figure 3**A simulates the distribution of magnetic field in the *YZ*- and the *XY*-planes for magnets that are square and rectangular prisms. Figure 3B shows the centering and alignment of several components of different shapes above the bottom magnet. The schematic shown to the left of each pair of photographs is a view of the simulated magnetic field from above the bottom magnet overlaid with an outline of the levitating shape. In each case, the experimentally observed position in the *XY*-plane qualitatively overlaps with the shape of the energetic minima suggested by the patterns of the magnetic field. Figure S2 in the Supporting Information demonstrates additional control over the vertical position, orientation, and spacing between levitating objects obtained by varying the distance between the magnets.

Figure 4 illustrates the alignment and positioning of components using common optical elements (mirrors and filters). The components in this figure all levitate independently (i.e., each one was programmed to levitate at a specific position; there are no mechanical connections between them). This type of self-assembly has the useful feature that it also occurs in a completely closed container (see Figure S3 in the Supporting Information).

We fabricated the levitating mirrors in Figure 4A by layering reflective Mylar tape onto the surface of polymethylmethacrylate (PMMA). We then used labeling tape (top mirror in Figure 4A) and aluminum tape (bottom mirror in Figure 4A) to program the levitation height and tilt angle of each mirror (the Supporting Information details the fabrication). Because the magnets used here for MagLev were square, tilted mirrors in Figure 4A can have four equivalent configurations during levitation and do not necessarily spontaneously face with the reflective side towards the light source. Tilting the MagLev device breaks the symmetry of the system and makes it possible to rotate the levitating mirrors, so that the heaviest part of the mirrors faces the direction of tilt. Gentle releveling of the MagLev device then traps the mirrors in a specific orientation (see Figure S4 and Movie S1 in the Supporting Information for details).

We used colored (green, red, and black) PMMA to fabricate light filters (Figure 4B). Green PMMA transmits the light emitted by a green laser pointer, but absorbs the light from a red laser pointer; red PMMA transmits red light and absorbs green. A PMMA-based IR filter absorbs light emitted by both red and green laser pointers. Figure S5 in the Supporting Information gives additional examples of MagLev for arranging objects in 3D (mirrors, commercial lenses, and diffraction gratings).

The ability of MagLev to suspend objects without contact with solid surfaces is a useful characteristic for manipulating fragile and soft components. **Figure 5** demonstrates several examples of levitation of components made from soft polymers, wet papers, and even liquids. Figure 5A shows the levitation of droplets of benzyl alcohol of three different sizes (5, 25, 250 μL). The difference in refractive index between the aqueous paramagnetic medium ($n_D \approx 1.33$) and benzyl alcohol ($n_D = 1.54$) and the smooth curved fluidic interface between the two liquids enable these droplets to act as ball lenses and focus light. The volume of the droplet determines the focal length of the lens. MagLev makes it possible to orient and suspend soft sheets

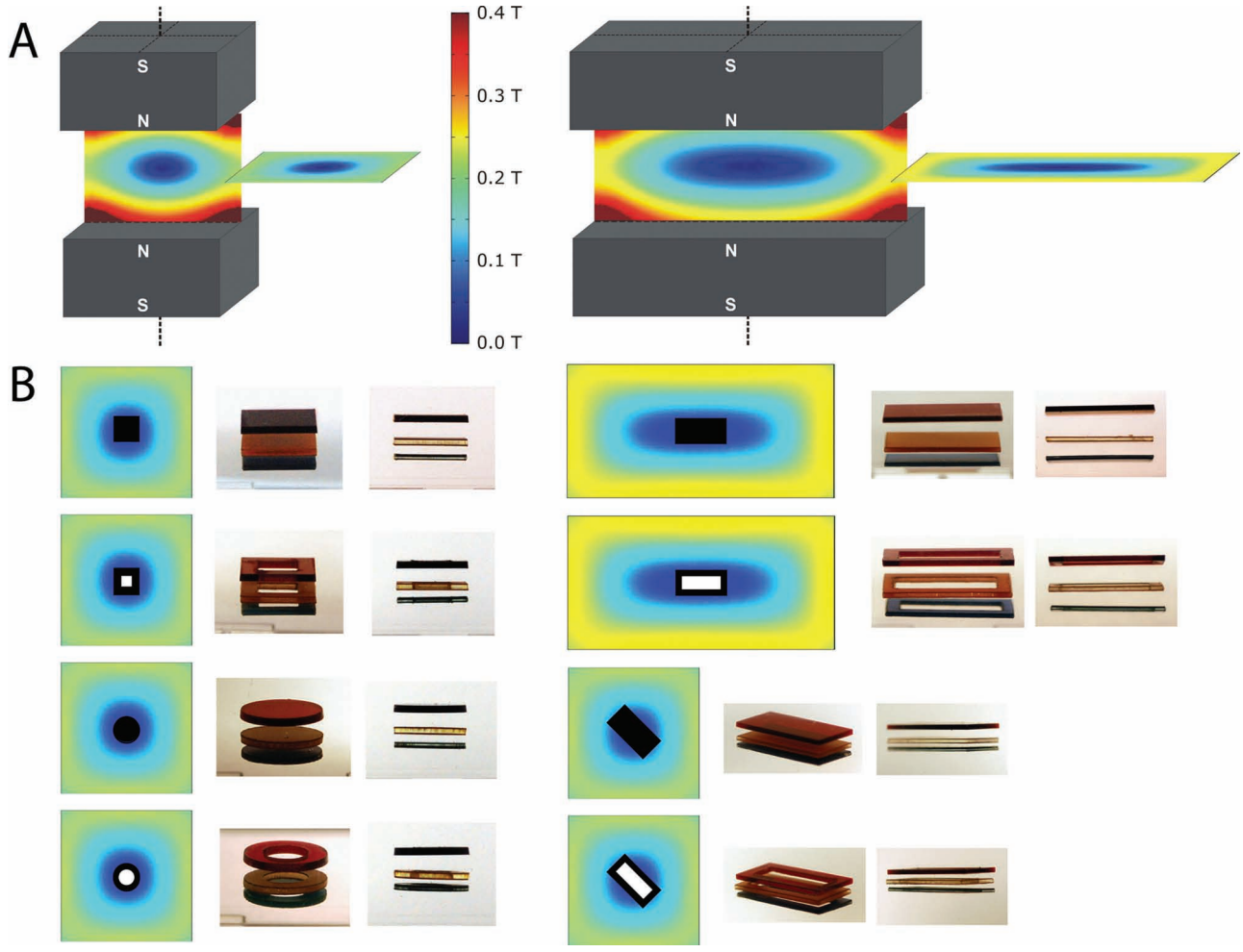

Figure 3. Controlling the position and orientation of objects with magnetic field gradients. A) COMSOL Multiphysics simulation of the magnetic field in the *YZ*- and *XY*-planes for two shapes of magnets (square prisms with dimensions of 50 mm × 50 mm × 25 mm, and rectangular prisms with dimensions of 100 mm × 50 mm × 25 mm) separated by $d = 35$ mm. The magnitude of the magnetic field in the simulations is constrained between 0 T and 0.4 T. B) Schematic representations (left), and photographs (center and right) demonstrating alignment and positioning in the *XY*-plane of shapes with different densities (fabricated from layers of PMMA and PVC; 10 mm in length or diameter; color-coded by density) levitating in 1.5 M aqueous $MnCl_2$. The schematic representation shown on the left demonstrates the top view (above the face of the bottom magnet) of the observed alignment of each shape in the magnetic field gradient of the *XY*-plane. The distribution of forces in the *XY*-plane determines the orientation of these objects with respect to the face of the bottom magnet. The photographs show an oblique view (center) and side view (right) of three levitating objects with indistinguishable shape but different density.

of wet paper on top of one another (Figure 5B); it also enables levitation of cotton thread in a linear conformation (Figure 5C). Figure 5D illustrates the ability to combine soft and rigid components during levitation and shows a droplet of 2-nitrotoluene levitating between two rigid PMMA-based disks. Draining of paramagnetic fluid from the container collapses the two disks onto the droplet.

By positioning and aligning components in 3D, MagLev makes it possible to assemble multicomponent structures. The process involves two stages: i) the balance of magnetic and gravitational forces acting on each of the components orders them into layered structures that are freely suspended in the paramagnetic liquid and ii) draining the liquid from the container stacks the components. **Figure 6** shows two demonstrations: the assembly of concentric circles on top of a supporting base (Figure 6A and Movie S2) and the assembly of four interlocking components (Figure 6B). In each demonstration, the individual components were programmed based on their densities to levitate at specific heights and to assemble into specific configurations based on shape. The shapes of the structures were designed using vector drawing software and fabricated by laser cutting from layers of PMMA and tape (see Supporting Information for details).

MagLev makes it possible to align, position, and assemble millimeter-scale components with heterogeneous density into functional 3D structures without physical contact. It is also possible to assemble and bring levitating components into contact by draining away the paramagnetic medium that suspends them.

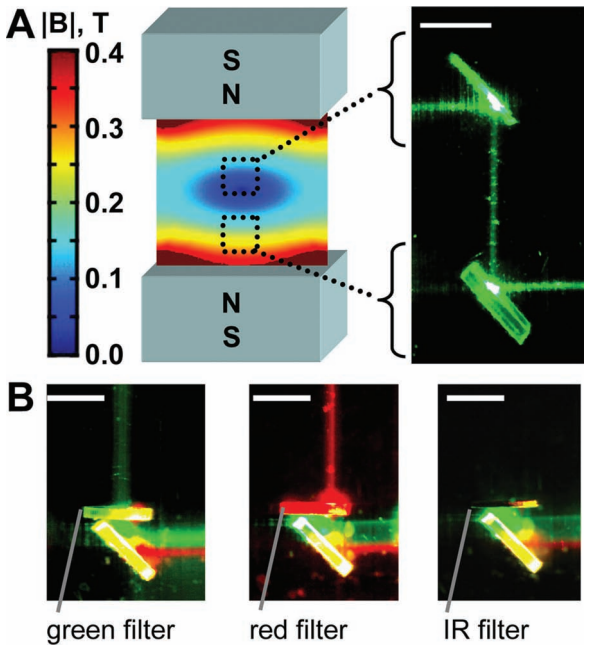

Figure 4. Photographs demonstrating alignment and positioning of optical components levitating in aqueous 1.5 M $MnCl_2$. Functionality of the optical system is illustrated by directing a laser at the assemblies. The scale bar in each photograph is 5 mm. A) Levitating mirrors guide the laser beam by reflection. B) A levitating mirror guides light through a filter. A green filter transmits the green light (left) and absorbs red; a red filter absorbs the green light and transmits red (middle); a PMMA-based IR filter absorbs both green and red light (right).

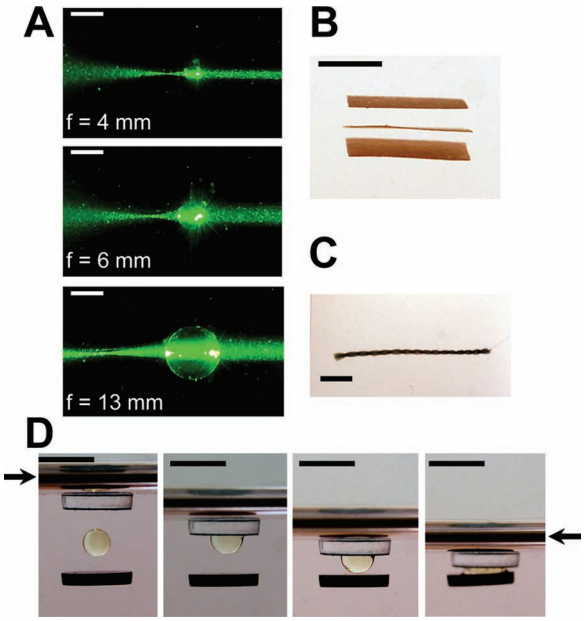

Figure 5. Photographs of levitating soft components. All scale bars are 5 mm in length. A) Three levitating droplets of various volumes of benzyl alcohol suspended in aqueous 0.35 M $MnCl_2$ (top: 5 µL, middle: 25 µL, and bottom: 250 µL) act as lenses and focus green light; the volume of the droplet controls the focal length (f) of the lens. B) Three layers of flat square cellulose-based sheets (top: nitrocellulose, middle: cellulose acetate, bottom: pure cellulose) levitating in aq. 3 M $MnCl_2$; the sheets maintain flat shape during levitation. C) A cotton thread assumes extended conformation during levitation in aq. 3 M $MnCl_2$. D) A droplet of 2-nitrotoluene sandwiched between two rigid polymeric disks. Draining of the paramagnetic fluid (aq. 1.5 M $MnCl_2$) from the container facilitates the collapse of the droplet between the two disks. The arrows indicate the air-liquid interface.

The technique has eight characteristics that make it especially suited for 3D self-assembly: i) It is rapid (millimeter-scale components reach their equilibrium configurations within seconds). ii) It is simple. Generating patterns of magnetic field gradient with permanent magnets and patterns of density with layers of polymers and adhesive is easy and inexpensive. iii) An easily tuned parameter, the density, directs objects into specific regions of 3D assemblies and controls their position and orientation in 3D space. iv) Changing the magnetic field changes the position and orientation of all components; a number of components can thus be manipulated in parallel. v) Because self-assembly takes place in a fluid, the components do not need to contact solid surfaces; moreover, fluidic suspension eliminates dry friction, stiction, contact adhesion, and static charging. vi) Self-assembly can proceed inside an entirely closed container. vii) Fragile or soft components (e.g., components made of gels, foams, soft plastics, or fluids) are compatible with MagLev. viii) External power is not required in many procedures.

The experimental approach described here also has three limitations: i) With the configuration of magnets used here, it is not possible to control the position of one component, independently of the others. The magnetic field acts on all components and perturbations tend to be non-local. ii) The objects that levitate in the current system using aqueous solutions of paramagnetic ions should have a density of $0.9 < \rho < 3$ g cm^{-3} (MagLev is, thus, not applicable to many solid metals, such as copper and gold) because the combined magnetic forces generated by the simple permanent magnets we have used are insufficient to balance the gravitational force on objects of density greater than ≈3 g cm^{-3}.[63] iii) It does not enable control over the positions of objects smaller than ≈5 micrometers in diameter because the magnetic and gravitational forces acting on these objects are insufficient to overcome Brownian motion for the configuration and type of magnets used in this study.[44,64]

MagLev offers an attractive approach for self-assembly in 3D for the orientation and assembly of components in an environment in which there is no solid-solid contact, for the protection of delicate components against shock and for the self-assembly of soft or fragile components. Strategies for programmable assembly using MagLev may be useful for aligning soft or deformable optical components, optical beam steering, and sensing applications.

Supporting Information

Supporting Information is available from the Wiley Online Library or from the author.

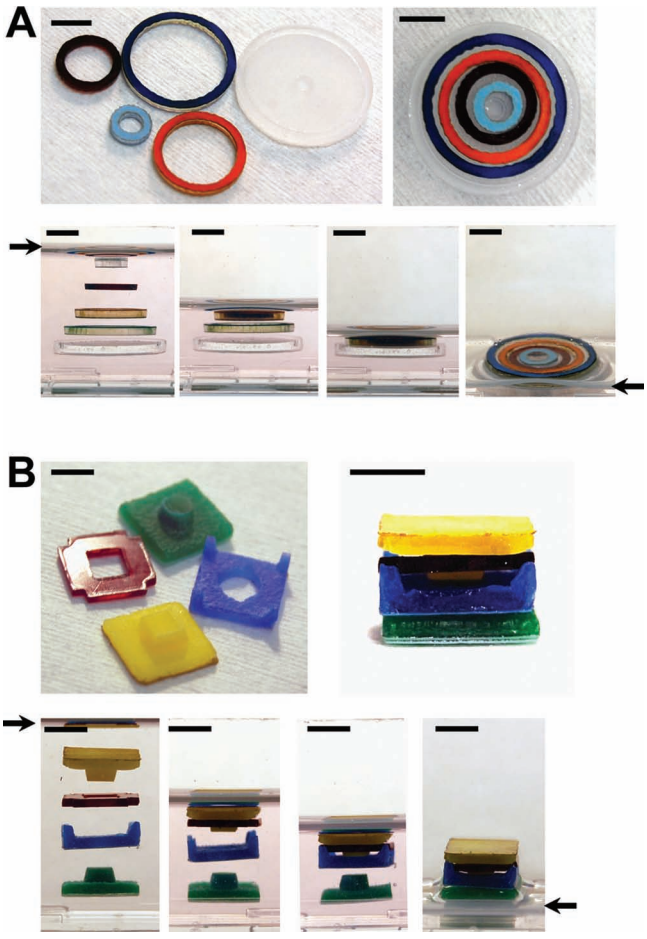

Figure 6. The assembly of multilayered structures by stacking in aq. 1.8 M $MnCl_2$. All scale bars are 5 mm in length. A) Photographs of four circles and a circular base before (top left), after (top right), and during (bottom) the assembly by MagLev. Draining the paramagnetic medium from the container while the system remained in the applied magnetic field lowered the air-liquid meniscus and deposited the centered, correctly sized concentric circles on top of the base. B) Photographs of four components designed to interlock upon assembly (top left: before assembly, top right: after assembly, bottom: during assembly). Draining of the paramagnetic fluid promotes stacking of the components into a layered structure. The arrows indicate the air-liquid interface.

Acknowledgements

This work was supported by DARPA award # W911NF-08-1-0143, Wyss Institute for Biologically Inspired Engineering, and the Ford Foundation (A. K. E.). K.A.M. thanks Darren J. Lipomi for discussions, Matthew R. Lockett for help with illustrations, and Rebecca Cademartiri and Ludovico Cademartiri for help with videos.

Received: May 23, 2011
Revised: June 22, 2011
Published online: August 10, 2011

[1] G. M. Whitesides, B. Grzybowski, *Science* **2002**, *295*, 2418.
[2] B. A. Grzybowski, C. E. Wilmer, J. Kim, K. P. Browne, K. J. M. Bishop, *Soft Matter* **2009**, *5*, 1110.
[3] Y. D. Yin, Y. Lu, B. Gates, Y. N. Xia, *J. Am. Chem. Soc.* **2001**, *123*, 8718.
[4] U. Srinivasan, D. Liepmann, R. T. Howe, *J. MEMS* **2001**, *10*, 17.
[5] Y. A. Vlasov, X. Z. Bo, J. C. Sturm, D. J. Norris, *Nature* **2001**, *414*, 289.
[6] J. D. Hartgerink, E. Beniash, S. I. Stupp, *Science* **2001**, *294*, 1684.
[7] J. C. Love, A. R. Urbach, M. G. Prentiss, G. M. Whitesides, *J. Am. Chem. Soc.* **2003**, *125*, 12696.
[8] M. Boncheva, D. A. Bruzewicz, G. M. Whitesides, *Pure Appl. Chem.* **2003**, *75*, 621.
[9] S. Srivastava, A. Santos, K. Critchley, K. S. Kim, P. Podsiadlo, K. Sun, J. Lee, C. L. Xu, G. D. Lilly, S. C. Glotzer, N. A. Kotov, *Science* **2010**, *327*, 1355.
[10] S. M. Douglas, H. Dietz, T. Liedl, B. Hogberg, F. Graf, W. M. Shih, *Nature* **2009**, *459*, 414.
[11] T. Liedl, B. Hogberg, J. Tytell, D. E. Ingber, W. M. Shih, *Nat. Nanotechnol.* **2010**, *5*, 520.
[12] R. M. Erb, H. S. Son, B. Samanta, V. M. Rotello, B. B. Yellen, *Nature* **2009**, *457*, 999.
[13] Z. H. Nie, A. Petukhova, E. Kumacheva, *Nat. Nanotechnol.* **2010**, *5*, 15.
[14] G. N. Meng, N. Arkus, M. P. Brenner, V. N. Manoharan, *Science* **2010**, *327*, 560.
[15] Y. N. Xia, B. Gates, Y. D. Yin, Y. Lu, *Adv. Mater.* **2000**, *12*, 693.
[16] D. H. Gracias, J. Tien, T. L. Breen, C. Hsu, G. M. Whitesides, *Science* **2000**, *289*, 1170.
[17] M. Boncheva, R. Ferrigno, D. A. Bruzewicz, G. M. Whitesides, *Angew. Chem. Int. Ed.* **2003**, *42*, 3368.
[18] M. Hashimoto, B. Mayers, P. Garstecki, G. M. Whitesides, *Small* **2006**, *2*, 1292.
[19] J. P. Ge, Y. X. Hu, Y. D. Yin, *Angew. Chem. Int. Ed.* **2007**, *46*, 7428.
[20] S. E. Chung, W. Park, S. Shin, S. A. Lee, S. Kwon, *Nat. Mater.* **2008**, *7*, 581.
[21] X. Y. Guo, H. Li, B. Y. Ahn, E. B. Duoss, K. J. Hsia, J. A. Lewis, R. G. Nuzzo, *Proc. Natl. Acad. Sci. USA* **2009**, *106*, 20149.
[22] E. M. Freer, O. Grachev, X. F. Duan, S. Martin, D. P. Stumbo, *Nat. Nanotechnol.* **2010**, *5*, 525.
[23] A. Dong, J. Chen, P. M. Vora, J. M. Kikkawa, C. B. Murray, *Nature* **2010**, *466*, 474.
[24] R. J. Knuesel, H. O. Jacobs, *Proc. Natl. Acad. Sci. USA* **2010**, *107*, 993.
[25] T. Fukushima, E. Iwata, T. Konno, J. C. Bea, K. W. Lee, T. Tanaka, M. Koyanagi, *Appl. Phys. Lett.* **2010**, *96*, 154105.
[26] M. Boncheva, S. A. Andreev, L. Mahadevan, A. Winkleman, D. R. Reichman, M. G. Prentiss, S. Whitesides, G. M. Whitesides, *Proc. Natl. Acad. Sci. USA* **2005**, *102*, 3924.
[27] E. Iwase, I. Shimoyama, *J. MEMS* **2005**, *14*, 1265.
[28] E. Iwase, I. Shimoyama, *Sens. Actuators A* **2006**, *127*, 310.
[29] R. Evrard, G.-A. Boutry, *J. Vac. Sci. Technol., A* **1969**, *6*, 279.
[30] B. R. F. Kendall, M. F. Vollero, L. D. Hinkle, *J. Vac. Sci. Technol., A* **1987**, *5*, 2458.
[31] E. Beaugnon, R. Tournier, *Nature* **1991**, *349*, 470.
[32] J. S. Brooks, J. A. Reavis, R. A. Medwood, T. F. Stalcup, M. W. Meisel, E. Steinberg, L. Arnowitz, C. C. Stover, J. Perenboom, *J. Appl. Phys.* **2000**, *87*, 6194.
[33] I. F. Lyuksyutov, D. G. Naugle, K. D. D. Rathnayaka, *Appl. Phys. Lett.* **2004**, *85*, 1817.
[34] I. Simon, A. G. Emslie, P. F. Strong, J. Robert K. McConnel, *Rev. Sci. Instrum.* **1968**, *39*, 1666.
[35] M. D. Simon, A. K. Geim, *J. Appl. Phys.* **2000**, *87*, 6200.
[36] R. T. Waldron, *Rev. Sci. Instrum.* **1966**, *37*, 29.
[37] A. T. Catherall, L. Eaves, P. J. King, S. R. Booth, *Nature* **2003**, *422*, 579.
[38] N. Hirota, M. Kurashige, M. Iwasaka, M. Ikehata, H. Uetake, T. Takayama, H. Nakamura, Y. Ikezoe, S. Ueno, K. Kitazawa, *Physica B* **2004**, *346*, 267.
[39] Y. Ikezoe, N. Hirota, J. Nakagawa, K. Kitazawa, *Nature* **1998**, *393*, 749.

[40] K. Yokoyama, N. Hirota, M. Iwasaka, *IEEE Trans. Appl. Appl. Supercond.* **2007**, *17*, 2181.
[41] U. Andres, *Magnetohydrodynamic & Magnetohydrostatic Methods of Mineral Separation*, John Wiley & Sons, New York, NY **1976**.
[42] T. Kimura, S. Mamada, M. Yamato, *Chem. Lett.* **2000**, 1294.
[43] I. F. Lyuksyutov, A. Lyuksyutova, D. G. Naugle, K. D. D. Rathnayaka, *Mod. Phys. Lett. B* **2003**, *17*, 935.
[44] K. A. Mirica, S. T. Phillips, C. R. Mace, G. M. Whitesides, *J. Agric. Food Chem.* **2010**, *58*, 6565.
[45] K. A. Mirica, S. T. Phillips, S. S. Shevkoplyas, G. M. Whitesides, *J. Am. Chem. Soc.* **2008**, *130*, 17678.
[46] K. A. Mirica, S. S. Shevkoplyas, S. T. Phillips, M. Gupta, G. M. Whitesides, *J. Am. Chem. Soc.* **2009**, *131*, 10049.
[47] T. Takayama, Y. Ikezoe, H. Uetake, N. Hirota, K. Kitazawa, *Appl. Phys. Lett.* **2005**, *86*.
[48] A. Winkleman, R. Perez-Castillejos, K. L. Gudiksen, S. T. Phillips, M. Prentiss, G. M. Whitesides, *Anal. Chem.* **2007**, *79*, 6542.
[49] E. Feinstein, M. Prentiss, *J. Appl. Phys.* **2006**, *99*, 064901.
[50] W. Braunbek, *Z. Phys.* **1939**, *112*, 753.
[51] I. Simon, U.S. Patent 3,465,598, **1969**.
[52] E. Beaugnon, R. Tournier, *J. Phys. III* **1991**, *1*, 1423.
[53] A. T. Catherall, P. Lopez-Alcaraz, K. A. Benedict, P. J. King, L. Eaves, *New J. Phys.* **2005**, *7*, 118.
[54] M. Hamai, I. Mogi, S. Awaji, K. Watanabe, M. Motokawa, *Jpn. J. Appl. Phys.* **2001**, *40*, 1336.
[55] N. Hirota, T. Takayama, E. Beaugnon, Y. Saito, T. Ando, H. Nakamura, S. Hara, Y. Ikezoe, H. Wada, K. Kitazawa, *J. Magn. Magn. Mater.* **2005**, *293*, 87.
[56] Y. Ikezoe, T. Kaihatsu, S. Sakae, H. Uetake, N. Hirota, K. Kitazawa, *Energy Conv. Manag.* **2002**, *43*, 417.
[57] I. Mogi, S. Takahashi, S. Awaji, K. Watanabe, M. Motokawa, *J. Phys.: Conf. Series* **2006**, *51*, 431.
[58] J. M. Valles, K. Lin, J. M. Denegre, K. L. Mowry, *Biophys. J.* **1997**, *73*, 1130.
[59] M. Yamato, H. Nakazawa, T. Kimura, *Langmuir* **2002**, *18*, 9609.
[60] H. Chetouani, C. Jeandey, V. Haguet, H. Rostaing, C. Dieppedale, G. Reyne, *IEEE Trans. Magn.* **2006**, *42*, 3557.
[61] A. Winkleman, K. L. Gudiksen, D. Ryan, G. M. Whitesides, D. Greenfield, M. Prentiss, *Appl. Phys. Lett.* **2004**, *85*, 2411.
[62] $MnCl_2$ and $GdCl_3$ are also soluble in alcohols and polar organic solvents, such as *N*,*N*-dimethylformamide and dimethylsulfoxide. A hydrophophobic Gd(III) chelate reported in ref. [44] also dissolves in a variety of organic solvents, and offers additional options for paramagnetic media that can be used for MagLev.
[63] It should be possible to overcome this limitation using a number of strategies, such as paramagnetic fluids with higher density, and/or higher magnetic susceptibility, as well as stronger magnetic fields.
[64] It should be possible to improve the levitation of small objects by using higher gradients of the magnetic field, e.g., by positioning magnets much more closely together.